Disease Models & Mechanisms 6, 95-105 (2013) doi:10.1242/dmm.010116

A zebrafish model of congenital disorders of glycosylation with phosphomannose isomerase deficiency reveals an early opportunity for corrective mannose supplementation

Jaime Chu[1,2,3], Alexander Mir[2,3], Ningguo Gao[4], Sabrina Rosa[2,3], Christopher Monson[2,3], Vandana Sharma[5], Richard Steet[6], Hudson H. Freeze[5], Mark A. Lehrman[4] and Kirsten C. Sadler[2,3,*]

SUMMARY

Individuals with congenital disorders of glycosylation (CDG) have recessive mutations in genes required for protein N-glycosylation, resulting in multi-systemic disease. Despite the well-characterized biochemical consequences in these individuals, the underlying cellular defects that contribute to CDG are not well understood. Synthesis of the lipid-linked oligosaccharide (LLO), which serves as the sugar donor for the N-glycosylation of secretory proteins, requires conversion of fructose-6-phosphate to mannose-6-phosphate via the phosphomannose isomerase (MPI) enzyme. Individuals who are deficient in MPI present with bleeding, diarrhea, edema, gastrointestinal bleeding and liver fibrosis. MPI-CDG patients can be treated with oral mannose supplements, which is converted to mannose-6-phosphate through a minor complementary metabolic pathway, restoring protein glycosylation and ameliorating most symptoms, although liver disease continues to progress. Because *Mpi* deletion in mice causes early embryonic lethality and thus is difficult to study, we used zebrafish to establish a model of MPI-CDG. We used a morpholino to block *mpi* mRNA translation and established a concentration that consistently yielded 13% residual Mpi enzyme activity at 4 days post-fertilization (dpf), which is within the range of MPI activity detected in fibroblasts from MPI-CDG patients. Fluorophore-assisted carbohydrate electrophoresis detected decreased LLO and N-glycans in *mpi* morphants. These deficiencies resulted in 50% embryonic lethality by 4 dpf. Multi-systemic abnormalities, including small eyes, dysmorphic jaws, pericardial edema, a small liver and curled tails, occurred in 82% of the surviving larvae. Importantly, these phenotypes could be rescued with mannose supplementation. Thus, parallel processes in fish and humans contribute to the phenotypes caused by Mpi depletion. Interestingly, mannose was only effective if provided prior to 24 hpf. These data provide insight into treatment efficacy and the broader molecular and developmental abnormalities that contribute to disorders associated with defective protein glycosylation.

INTRODUCTION

Congenital disorders of glycosylation (CDG) are rare, under-diagnosed monogenic disorders with over 1000 affected individuals identified worldwide (Freeze, 2006; Freeze et al., 2012; Haeuptle and Hennet, 2009; Jaeken, 2010). CDG is caused by mutation of genes required for N-linked protein glycosylation; of 38 distinct subtypes, only one has a broadly effective treatment option. Mutation in genes that encode enzymes or cofactors necessary to synthesize the lipid-linked oligosaccharide (LLO), the major precursor of N-linked glycoproteins, and its transfer to acceptor proteins in the ER (Kornfeld and Kornfeld, 1985) defines those individuals considered 'type I', whereas type II is defined as those mutations that affect genes involved in processing the oligosaccharide after it is transferred to the protein.

Early in life, individuals with type I CDG typically develop protein hypoglycosylation and multi-systemic pathologies, including cardiac, neurological, musculoskeletal, gastrointestinal and hepatic disease with high morbidity and mortality (Freeze, 2001; Freeze et al., 2012; Jaeken et al., 1980). It is thought that insufficient LLO production is the basis of this disease. In fact, although the genetic and clinical defects of hypoglycosylation that accompany most CDG are well characterized, the cellular and developmental abnormalities that cause pathology are poorly understood. Development of whole animal models to study different types of CDG will allow this to be addressed.

Mannose phosphate isomerase (MPI) is required to convert fructose-6-phosphate to mannose-6-phosphate (Fig. 1A). Individuals with MPI-CDG primarily develop gastrointestinal problems, including diarrhea caused by protein-losing enteropathy, gastrointestinal bleeding due to coagulopathy resulting from failed hepatocyte secretion or instability of clotting factors (which are glycoproteins), and underlying portal hypertension caused by congenital hepatic fibrosis (de Lonlay and Seta, 2009; Freeze, 2001). MPI-CDG is the only CDG with a known treatment: oral mannose

[1]Division of Pediatric Hepatology/Department of Pediatrics, [2]Division of Liver Diseases/Department of Medicine, [3]Department of Developmental and Regenerative Biology, Mount Sinai School of Medicine, New York, NY 10029, USA
[4]Department of Pharmacology, University of Texas Southwestern Medical Center, Dallas, TX 75390, USA
[5]Sanford Children's Health Research Center, Sanford-Burnham Medical Research Institute, La Jolla, CA 92037, USA
[6]Complex Carbohydrate Research Center, University of Georgia, Athens, GA 30602, USA
*Author for correspondence (kirsten.edepli@mssm.edu)

Received 23 April 2012; Accepted 29 June 2012

TRANSLATIONAL IMPACT

Clinical issue

Congenital disorders of glycosylation (CDG) are rare, under-diagnosed genetic disorders, with ~1000 affected individuals identified worldwide. Individuals with CDG carry mutations in genes required for proper N-linked protein glycosylation (including in *MPI*, encoding an essential enzyme in the glycosylation pathway) and have multi-systemic pathologies, including cardiac, neurological, musculoskeletal, gastrointestinal and hepatic disease, as well as high rates of morbidity and mortality. Of 38 distinct subtypes, only one has a broadly effective treatment option. The genetic and clinical defects of hypoglycosylation that accompany most CDG are well characterized, but the cellular and developmental abnormalities that cause pathology are poorly understood. Zebrafish models of CDG will provide much-needed tools, because the development of mice with hypomorphic alleles is costly and time consuming. In addition, mouse models generated thus far have failed to adequately replicate the abnormal gene expression, developmental abnormalities, protein hypoglycosylation and loss of lipid-linked oligosaccharides (LLOs; the sugar donor for glycosylation events) that are associated with the human disease.

Results

This study presents the first zebrafish model of CDG. Using morpholinos to block expression of MPI, an enzyme that is essential for glycosylation, the authors demonstrate that zebrafish *mpi* morphants display pathologies that are comparable to those present in CDG individuals carrying *MPI* mutations (MPI-CDG) – including depleted LLO and mannose 6-phosphate levels, increased embryonic mortality and phenotypic abnormalities. Importantly, these abnormalities can be rescued with mannose supplementation, the mainstay of therapy for individuals with MPI-CDG.

Implications and future directions

This zebrafish model is the first free-living in vivo model to study MPI-CDG, and provides proof-of-principle that zebrafish can be used to study other CDG and disorders of glycosylation. It is hoped that this will serve as a platform to further investigate the pathophysiology underlying these disorders and, ultimately, to facilitate therapeutic screening.

increases the flux of mannose into the depleted glycosylation pathway by relying on hexokinase, through a minor complementary metabolic pathway, to produce mannose-6-phosphate and bypass the MPI deficiency (Fig. 1A). Mannose treatment improves defective protein glycosylation in patients and ameliorates most, but not all, symptoms: liver disease continues to progress (Mention et al., 2008; Miller et al., 2009; Niehues et al., 1998). Furthermore, the ideal window for mannose treatment has not been clearly established.

MPI-CDG alleles are typically hypomorphic and *Mpi* null mice die in utero at 11.5 days post-coitum (DeRossi et al., 2006), indicating that complete loss of this enzyme is not compatible with survival. Zebrafish (*Danio rerio*) are a powerful and complementary vertebrate system in which to study monogenic disorders, largely owing to their high genetic conservation with humans and the ability to carry out reverse genetics using morpholino-mediated knockdown in these animals. Human MPI is 63% identical to the zebrafish protein and biochemical assays used for measuring MPI activity in mammals can be easily applied to extracts from zebrafish. Morpholinos block protein translation and can be titrated, allowing us to precisely monitor efficacy of knockdown by direct biochemical measurement of Mpi enzyme activity. Zebrafish models of CDG will provide much-needed tools to study CDG pathology because development of mice with hypomorphic alleles is costly and time consuming, and the mice generated thus far have failed to adequately replicate the abnormal gene expression, developmental abnormalities, protein hypoglycosylation and loss of LLOs associated with the human disease.

In zebrafish, hundreds of embryos can be injected in each experiment, providing ample material for biochemical experiments and statistical power for phenotypic analysis. Large clutches and rapid development in a transparent embryo allows for large-scale, inexpensive, real-time analysis of development and disease progression. Within 5 days post-fertilization (dpf), larvae have emerged from their chorion, have consumed the maternally provided yolk and are ready to feed, with their neural, musculoskeletal and digestive systems fully established and functional (Chu and Sadler, 2009; Lieschke and Currie, 2007; Mudbhary and Sadler, 2011).

Here, we demonstrate that zebrafish *mpi* morphants display biochemical and morphological features of MPI-CDG patients, including depleted LLO and mannose 6-phosphate accompanied by increased mortality as well as hepatic and other phenotypic abnormalities. Importantly, these abnormalities can be treated with mannose supplementation, the mainstay of therapy for individuals with MPI-CDG. Thus, zebrafish provide a novel system in which to study CDG. Moreover, although CDG are rare, the liver and gastrointestinal manifestations such as liver fibrosis or protein-losing enteropathy that individuals with CDG develop are shared by patients with more common causes of these same manifestations. An understanding of the cellular defects in CDG that give rise to pathology are particularly relevant to the broader field of liver disease, because non-alcoholic fatty liver disease, fibrosis and cirrhosis have all been associated with defects in protein glycosylation (Blomme et al., 2009).

RESULTS

mpi morpholino injection decreases Mpi activity in zebrafish embryos

MPI-CDG patients typically have hypomorphic mutations in the *MPI* gene, resulting in decreased, but not total loss, of MPI activity. Moreover, *Mpi* knock-out mice die in utero (DeRossi et al., 2006), whereas heterozygous humans and mice lack detectable abnormalities. This suggests that a complete loss of MPI is not compatible with survival, whereas heterozygosity for MPI is well tolerated. Thus, we sought to develop a model of MPI-CDG in zebrafish by using morpholinos to decrease the residual Mpi activity to less than 20% of controls, reflecting the range of Mpi activity from 3% to 18% of controls detected in MPI-CDG patient leukocytes, cultured fibroblasts and liver tissue (Babovic-Vuksanovic et al., 1999; de Koning et al., 1998; de Lonlay et al., 1999; Jaeken et al., 1998; Kjaergaard, 2004; Niehues et al., 1998; Westphal et al., 2001).

To block translation of *mpi* mRNA, a morpholino (MO) targeting the initiator ATG of zebrafish *mpi* mRNA (supplementary material Table S1) was injected in amounts ranging from 0.3-13 ng per embryo. We found ~10-12% mortality prior to 24 hours post-fertilization (hpf) in uninjected embryos or those injected with a standard control morpholino (predicted to have no direct targets in zebrafish), but there was little to no mortality on subsequent days (supplementary material Fig. S1). In contrast, concentrations of *mpi* morpholino exceeding 3.35 ng per embryo resulted in significant

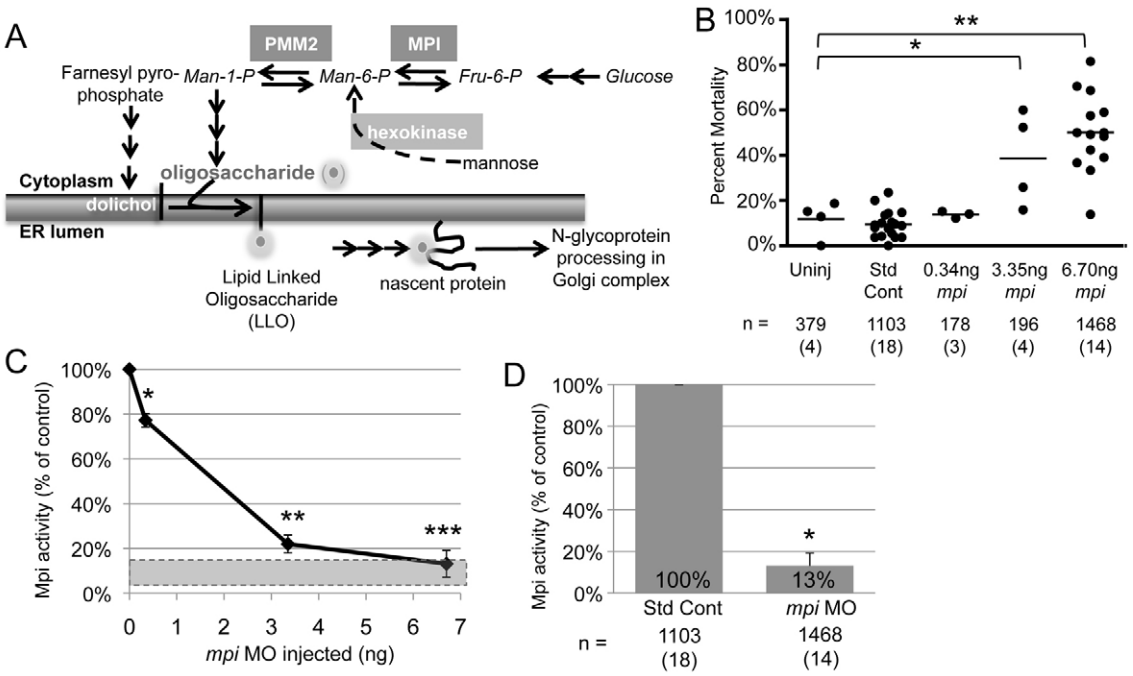

Fig. 1. Titration of *mpi* morpholino results in dose-dependent mortality and Mpi enzyme knockdown. (A) Abridged schematic of N-glycosylation focused on the MPI and PMM2 enzymatic steps. (B) Zebrafish embryos were injected with *mpi* ATG blocking morpholino (MO) and collected at 4 days post-fertilization (dpf). Cumulative mortality on 4 dpf for the increasing amounts of *mpi* MO injected are shown. * and **, $P<0.0001$ by Fisher's exact test. Numbers in parentheses under *n* values indicate the number of experiments. (C) Mpi activity was measured in 4 dpf lysates (normalized to total protein) using the standard coupled assay for this enzyme. Mpi activity expressed as the percent of control activity is shown. Gray bar indicates the range of Mpi activity demonstrated in MPI-CDG individuals (3-18%). *P=0.04; **P=7.52E–06; ***P=1.38E–18 by unpaired *t*-test. (D) Mpi enzyme activity is 13% (as compared with standard control MO) when 6.7 ng of *mpi* MO is injected. *$P<0.0001$ by Fisher's exact test.

mortality during the first 4 dpf (Fig. 1B and supplementary material Fig. S1). On average, 20% mortality of *mpi* morphants occurred by 24 hpf and 50% of embryos injected with 6.7 ng morpholino were dead by 4 dpf, with a range of 14-81% mortality across 14 experiments (Fig. 1B; $P<0.0001$ by Fisher's exact test). Thus, in zebrafish and in mammals, Mpi is essential for normal embryogenesis.

We measured Mpi enzyme activity in whole lysates obtained from 4 dpf larvae injected with a range of morpholino concentrations with over 50% cumulative survival and in larvae injected with a standard control morpholino at the same concentration (Fig. 1C). There was no difference between uninjected larvae and those injected with the standard control morpholino, with median units of Mpi activity at 13.6 and 14.6, respectively (supplementary material Table S2). Increasing concentrations of *mpi* morpholino effectively reduced the amount of Mpi activity in 4 dpf larvae: 0.34, 3.35 and 6.7 ng of *mpi* morpholino reduced Mpi activity to 10.71, 3.05 and 1.83 units, respectively (supplementary material Table S2), corresponding to 77, 22 and 13% residual activity (Fig. 1C). Importantly, on average, in over 14 separate experiments, 6.7 ng of morpholino reduced Mpi activity to 13% in 4 dpf larvae (Fig. 1D), which is within the range of residual activity detected in MPI-CDG patient cells (Babovic-Vuksanovic et al., 1999; de Koning et al., 1998; de Lonlay et al., 1999; Jaeken et al., 1998; Kjaergaard, 2004; Niehues et al., 1998; Westphal et al., 2001). There was no appreciable increase in Mpi activity by 5 dpf (supplementary material Fig. S2A), suggesting sustained morpholino efficacy.

The effect of Mpi loss on phosphomannomutase 2 (Pmm2), the next downstream enzyme in the mannose metabolism pathway (Fig. 1A), was assayed. We found a modest reduction in residual Pmm2 activity in *mpi* morphants at 4 dpf (86% of controls; P=0.011 by paired *T*-test; supplementary material Fig. S2B). We speculate that this is caused by reduced size of the organs that express high *mpi* and *pmm2* levels, such as the brain, gut and liver (Thisse and Thisse, 2004) in severely affected *mpi* morphants. However, the dramatic increase in the Pmm2:Mpi ratio from 0.4 in controls to over 2.7 in *mpi* morphants (supplementary material Fig. S2C) indicates that depletion of Mpi exceeds any non-specific effects. The specific activities of both Mpi and Pmm2 (in mU/mg protein) and the relative ratios of these enzymes are similar to those measured in humans and mouse samples (de Lonlay et al., 1999; Freeze, 2009; Niehues et al., 1998; Van Schaftingen and Jaeken, 1995), suggesting that the level of cellular enzymatic activity of these enzymes is conserved across species.

mpi knockdown in zebrafish embryos causes defects in LLO synthesis

Mannose is one of the core sugar building blocks to form the mature LLO, which is used as the oligosaccharide donor for modification of secretory proteins on asparagine residues (i.e. N-linked glycosylation). The function of MPI in N-glycosylation is to produce mannose-6-phosphate (Fig. 1A). Mannose-6-phosphate is then converted to mannose-1-phosphate by PMM2, and subsequently to GDP-mannose, which is used as the substrate for generating the

mature LLO. Thus, individuals with MPI and PMM2 deficiencies are predicted to have decreased LLO levels, although this has not been directly tested in patient samples or in any CDG animal models.

We hypothesized that Mpi deficiency in our morphants would result in defects in LLO synthesis because of decreased mannose-6-phosphate levels. To test this, fluorophore-assisted carbohydrate electrophoresis (FACE) analysis was used to measure mature LLO [$G_3M_9Gn_2$-P-P-dolichol (G_3M_9); oligosaccharide containing three glucose, nine mannose, two N-acetylglucosaminylpyrophosphoryl dolichol] and mannose-6-phosphate levels in 4 dpf *mpi* morphants compared with larvae injected with the standard control morpholino. Indeed, both mature (G_3M_9) LLO and mannose-6-phosphate levels were decreased by an average of 47 and 41%, respectively (Fig. 2A,B). This is comparable to what was detected in larvae treated from 3 to 5 dpf with 1 µg/ml of tunicamycin, another means to prevent the formation of mature LLO (Fig. 2B). In addition to FACE analysis, mannose-6-phosphate content in embryos was further confirmed using a coupled enzyme assay (supplementary material Fig. S2D). Moreover, *mpi* morphants had a 47±9.2% (s.e.m., n=2) decrease of total N-linked glycans, a result that is consistent with the identification of hypoglycosylated serum glycoproteins in MPI-CDG patients (Fig. 2C). Thus, Mpi knockdown reduces LLO levels and this presumably reduces the precursor available for protein modification, resulting in a decrease in the global levels of N-linked sugar moieties. No selective increases of particular LLO intermediates in the M_5Gn_2-P-P-dolichol to $G_2M_9Gn_2$-P-P-dolichol range were detected (Fig. 2A). Together, these data indicate that morpholino-mediated knockdown of Mpi results in significant depletion of Mpi activity and mannose-6-phosphate levels. These are directly correlated with decreased mature LLO formation and result from an abnormality preceding the step that generates the M_5Gn_2-P-P-dolichol intermediate.

mpi morphants develop multi-systemic abnormalities

Individuals with CDG commonly exhibit musculoskeletal, neurological, hepatic and gastrointestinal abnormalities that contribute to the substantial morbidity associated with this disorder (Freeze, 2001; Freeze, 2006; Freeze et al., 2012; Haeuptle and Hennet, 2009; Jaeken et al., 1980; Kjaergaard, 2004). We analyzed *mpi* morphants for phenotypic abnormalities induced by Mpi depletion. We found no appreciable difference in mortality (Fig. 1B and supplementary material Fig. S1), Mpi activity (supplementary material Table S2) or morphology between uninjected larvae and those injected with 6.7 ng of control morpholino, and less than 10% of either uninjected or control-morpholino-injected embryos displayed any developmental delay or visible abnormality (categorized as miscellaneous). However, specific phenotypes developed in *mpi* morphants that we categorized as mild or severe. Other than a moderate increase in mortality, there were no consistent morphological defects observed at 24 hpf. The mild phenotype was first detectable at 2 dpf as a mild microphthalmia and reduced forebrain size that persisted through 4 dpf and was accompanied by a slight tail curvature, abnormally shaped jaw, small liver and under utilization of yolk. These phenotypes were more exaggerated in severely affected larvae, which had the additional phenotype of severe lordosis and pericardial edema (Fig. 3A, bottom panels, and supplementary material Fig. S3). There was clutch-to-clutch variation in the percent of morphants that were normal (from 0 to 35% with a normal phenotype), but the average among 13 clutches was 15% (Fig. 3B; P<0.0001 by Fisher's exact test). On average, of the morphants that survived to 4 dpf, 85% showed an abnormal phenotype with 52% of them demonstrating a severe phenotype. We speculate that unaffected larvae resulted from technical variability or to stochastic modifiers of the phenotype.

Individuals with MPI-CDG commonly develop hepatic disease, and we thus investigated whether the liver was affected in *mpi* morphants. Liver size was scored in live larvae expressing dsRed in hepatocytes [*Tg(fabp10:dsRed)*]. On 4 dpf, when the control liver can clearly be observed as a large oblong or crescent-shaped organ anterior to the intestinal bulb, all morphants classified as severe, most of those classified as mild and even some larvae that were scored as phenotypically normal had a small liver (Fig. 3A,C). On average, over 75% of *mpi* morphants had a small liver. Thus, liver development is highly sensitive to Mpi loss.

We developed a scoring system to further quantify the severity of the affected clutch (i.e. a 'phenotype score,' described in Methods) to enable quantification of clutch-to-clutch variation and to correlate the range in phenotype and severity of each clutch to the degree of residual Mpi enzyme activity (Fig. 3D). We hypothesized

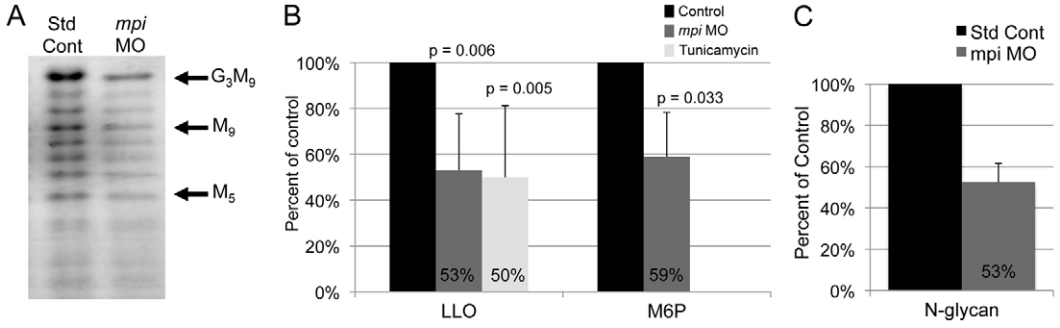

Fig. 2. Mpi knockdown decreases full-length LLO and mannose-6-phosphate levels in zebrafish. (A) Full-length LLO (G_3M_9) levels are decreased by Mpi knockdown, as seen on FACE analysis. (B) G_3M_9 LLO (normalized to number of fish) and mannose-6-phosphate (M6P) levels (normalized to 100 microgram protein) in lysates from 4 dpf zebrafish larvae. Values from larvae injected with the standard control morpholino were set as 100%. Average from three experiments. (C) N-glycans are decreased to 53% in *mpi* morphants on FACE analysis as compared with standard controls (n=2 experiments).

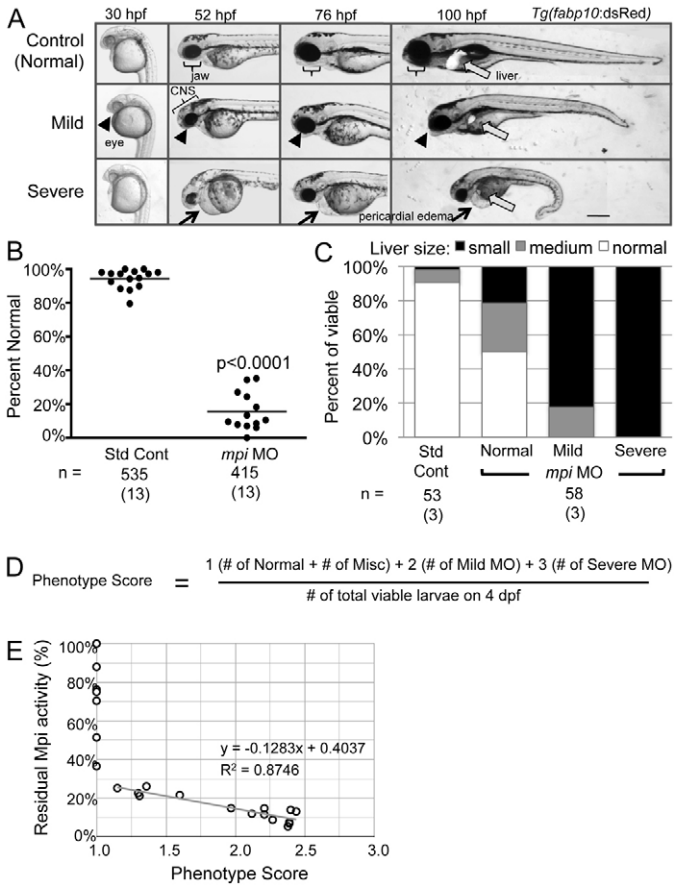

Fig. 3. *mpi* morphants develop multi-systemic abnormalities. (A) Injection of 6.7 ng of *mpi* MO results in morphants that are characterized by a small head, microphthalmia, pericardial edema, jaw defects and reduced liver size as visualized in live fish expressing dsRed in hepatocytes [*Tg(fabp10:*dsRed*)*] from 30 to 100 hpf. Scale bar: 50 µm. (B) Embryo clutches injected with *mpi* MO have an average of 15% phenotypically normal embryos as compared with 93% of control embryos. Range from 0-35% normal. $P<0.0001$ by Fisher's exact test. Numbers in parentheses under *n* values indicate the number of experiments. (C) Injection of 6.7 ng of *mpi* MO results in abnormal liver development. Liver size correlated with severity of phenotype. (D) 'Phenotype score' equation. (E) Linear regression analysis shows that phenotype score is inversely correlated with residual Mpi enzyme activity.

that the phenotype score would be inversely correlated with the amount of residual Mpi activity in each clutch, i.e. the most severe phenotype would be associated with the greatest knockdown. This was supported by a significant linear correlation between severity of phenotype and Mpi activity (R^2=0.87; Fig. 3E).

We confirmed that the effect of the *mpi* morpholino was not attributed to an off-target or non-specific toxic effect as described for other morpholinos (Ekker and Larson, 2001; Robu et al., 2007) by rescuing the phenotype with co-injection of *mpi* mRNA. The cDNA was created using primers that incorporated degeneracy surrounding the ATG, and was tagged with an N-terminal *6×-myc* epitope to prevent binding of morpholino directed against the endogenous *mpi* mRNA (supplementary material Table S1). Following injection of *6×-myc-mpi* mRNA, immunoblotting demonstrated that Mpi persisted until 4 dpf (Fig. 4A), Mpi enzyme activity was restored (Fig. 4B) and *mpi* morphant phenotype was rescued (Fig. 4C,D), so that 79% of embryos co-injected with *6×-myc-mpi* mRNA and *mpi* morpholino were completely normal, compared with 6% of those injected with the *mpi* morpholino alone (Fig. 4D; $P<0.0001$ by Fisher's exact test). Mortality was also improved with co-injection (31% mortality) as compared with the *mpi* morpholino group (48% mortality; $P=0.0007$ by Fisher's exact test). Thus, we conclude that the *mpi* morphant phenotype is caused by Mpi deficiency and not by an off-target morpholino effect. However, this did not rule out the formal possibility that the morphant phenotype was due to an absence of MPI polypeptide (perhaps acting as a scaffold or regulator) rather than an absence of its enzymatic activity per se. This was addressed by testing the effects of metabolic rescue using mannose.

Early addition of mannose rescues the *mpi* morphant phenotype

Of the 21 type I CDG, MPI-CDG is the only subtype with a clinically validated therapy for treatment. The first successful treatment of a 6-year-old MPI-CDG patient with oral mannose supplementation resulted in clinical response within 2 weeks and subsequent improvement in serum protein glycosylation pattern at an 11-month follow up (Niehues et al., 1998). Subsequently, additional reports have demonstrated successful mannose therapy in MPI-CDG patients (Damen et al., 2004; de Lonlay and Seta, 2009; Harms et al., 2002; Hendriksz et al., 2001; Mention et al., 2008; Penel-Capelle et al., 2003). Mannose supplementation is proposed to treat MPI-CDG by exploiting a normally minor metabolic pathway involving hexokinase, which can convert oral mannose to mannose-6-phosphate and thus bypass the deficiency of Mpi enzyme (Fig. 1A). This pathway is well conserved in vertebrates, with 86% identity between human and zebrafish hexokinase 1 proteins. Thus, we predicted that the phenotype and biochemical defects in Mpi-deficient larvae would be rescued with exogenous mannose if they were caused by a lack of mannose-6-phosphate.

To test this, mannose ranging from 0 to 50 mM was added to the fish culture media of *mpi* morphants and controls immediately after morpholino injection (at 1 hpf) and larvae were scored at 4 dpf (supplementary material Fig. S4A). Mannose supplementation significantly but modestly improved the cumulative *mpi* morphant mortality by 4 dpf (25% in treated compared with 20% in *mpi* morpholino alone; $P=0.043$ by Fisher's exact test). At 4 dpf, we found that 77% of *mpi* morphants treated with 50 mM mannose appeared completely normal, whereas no rescue was seen with glucose (Fig. 5A,B). The reduced liver size in *mpi* morphants was also significantly rescued with mannose supplementation (Fig. 5A,C). There was a slight, but not significant, increase in Mpi enzyme activity in mannose-treated morphants, which we predict might reflect the overall improved health of these larvae and the restoration of those organs that express the highest levels of *mpi* (Fig. 5D). Biochemical markers of N-glycosylation were also improved by mannose supplementation: mannose-6-phosphate and G_3M_9 LLO levels were restored in *mpi* morphants (Fig. 5E,F). Therefore, we conclude that 50 mM mannose provided just after fertilization effectively rescues the morphological and biochemical defects caused by Mpi deficiency.

We recently reported that elevated mannose-6-phosphate concentrations can cause LLO cleavage in mammalian tissue culture cells, suppressing steady-state LLO levels when rates of LLO

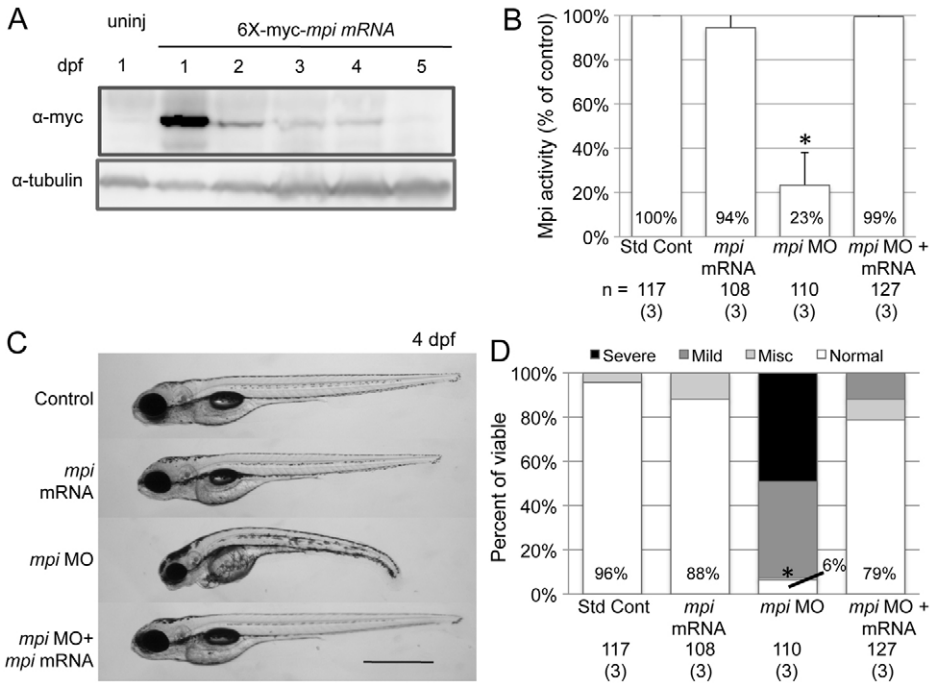

Fig. 4. *mpi* morphants are rescued with *mpi* mRNA. Full-length zebrafish *mpi* mRNA was cloned using degenerate sequencing primers surrounding the ATG site so that no significant overlap with MO sequence would occur. The embryos were injected with either standard control MO, *mpi* MO, *6×-myc-mpi* mRNA or *mpi* MO + *6×-myc-mpi* mRNA. (A) Western blot showing Mpi expression in embryos from 1 to 5 dpf after *mpi* mRNA injection at *t*=0. (B) Restoration of Mpi enzyme activity in embryos injected with either *mpi* mRNA only or co-injected with *mpi* MO + mRNA (P=0.47 and 0.80 by paired *t*-test, respectively, as compared with standard control MO). *P=0.047 by paired *t*-test. Results from three experiments. (C) *mpi* morphants show phenotypic rescue when co-injected with *6×-myc-mpi* mRNA. Scale bar: 50 µm. (D) At 4 dpf, 78% of morphants injected with *6×-myc-mpi* mRNA were rescued to normal as compared with 6% normal in *mpi* MO embryos; * P<0.0001 by Fisher's exact test. Numbers in parentheses under *n* values indicate the number of experiments.

resynthesis are insufficient (Gao et al., 2011; Gao et al., 2005; Gill et al., 2002). However, in zebrafish, despite the increase in mannose-6-phosphate levels in control embryos exposed to mannose, this was not sufficient to affect LLO levels (supplementary material Fig. S4B,C), suggesting that LLO synthesis under these conditions was sufficient to maintain steady-state levels of LLO.

The timing of mannose supplementation to achieve optimal efficacy for MPI-CDG patients is not known (de Lonlay and Seta, 2009; Westphal et al., 2001). Debate surrounding whether mannose supplements can eventually be reduced or whether life-long therapy is required remains unresolved. Indeed, although vast clinical improvement of MPI-CDG patients is achieved within weeks of mannose therapy, some complications, including hepatic fibrosis, persist and even can progress despite continued mannose supplementation (Mention et al., 2008). Thus, mannose therapy in MPI-CDG children, although a significant advance, does not completely resolve all disease manifestations. One possibility is that the defects that eventually lead to hepatic fibrosis occur prior to the time when mannose therapy is initiated.

We therefore sought to define the time when mannose addition was the most effective at rescuing *mpi* morphants. *mpi*-morpholino-injected embryos were treated with 50 mM mannose at 1 hpf and the mannose was subsequently removed at either 24, 48 or 72 hpf. Untreated morphants and those treated with mannose continually through 96 hpf as previously described in Fig. 5 were included as controls. All larvae were scored at 96 hpf. As expected, nearly all larvae injected with the control morpholino seemed to have no morphological abnormalities (99% normal), whereas, in this series of experiments, 32% of untreated *mpi* morphants were normal. Surprisingly, all durations of mannose exposure had the same effect: over 70% of *mpi* morphants appeared normal in all groups (Fig. 6A). Thus, the presence of mannose for only the first 24 hours was sufficient to rescue Mpi deficiency.

We next assessed the benefit of mannose supplementation in older embryos by adding mannose at later time points (24 and 48 hpf) and scored them at 96 hpf. Surprisingly, these treatments added later in embryonic development were unable to rescue the *mpi* phenotype (Fig. 6B). Together, these data show that mannose rescue corrects abnormalities only early in development and also indicates that subsequent phenotypic defects were later manifestations of the earliest disruptions. Given that in situ hybridization detected high *mpi* expression as early as gastrulation [~5.5 to 12.5 hpf (Thisse and Thisse, 2004)], we conclude that Mpi expression and activity is required for early embryogenesis.

The simple addition of mannose to the water, akin to the oral supplementation in MPI-CDG patients, and its remarkable rescue of the morphant phenotype serves to further confirm the specificity of phenotype induced by *mpi* morpholino injection. This validates zebrafish as a novel vertebrate system to study the effects of protein glycosylation defects and sugar metabolism on development and disease.

DISCUSSION

CDG is a collection of rare, under-diagnosed genetic disorders with gene mutations encoding enzymes necessary for protein N-glycosylation. The clinical spectrum of CDG patients ranges from moderate defects to devastating multi-systemic disease that carries high morbidity and mortality (Freeze, 2001; Jaeken et al., 1980). CDG patients represent over 38 distinct subtypes affecting nearly 1000 individuals worldwide. Unfortunately, MPI-CDG is the only subtype with a known treatment and this represents only a small fraction of all CDG patients. Here, we address the developmental consequences of glycosylation deficiency in zebrafish by depletion of Mpi. We validate this system as a novel model to study CDG-MPI by validating both the biochemical and phenotypic effects of Mpi loss in embryos and by demonstrating

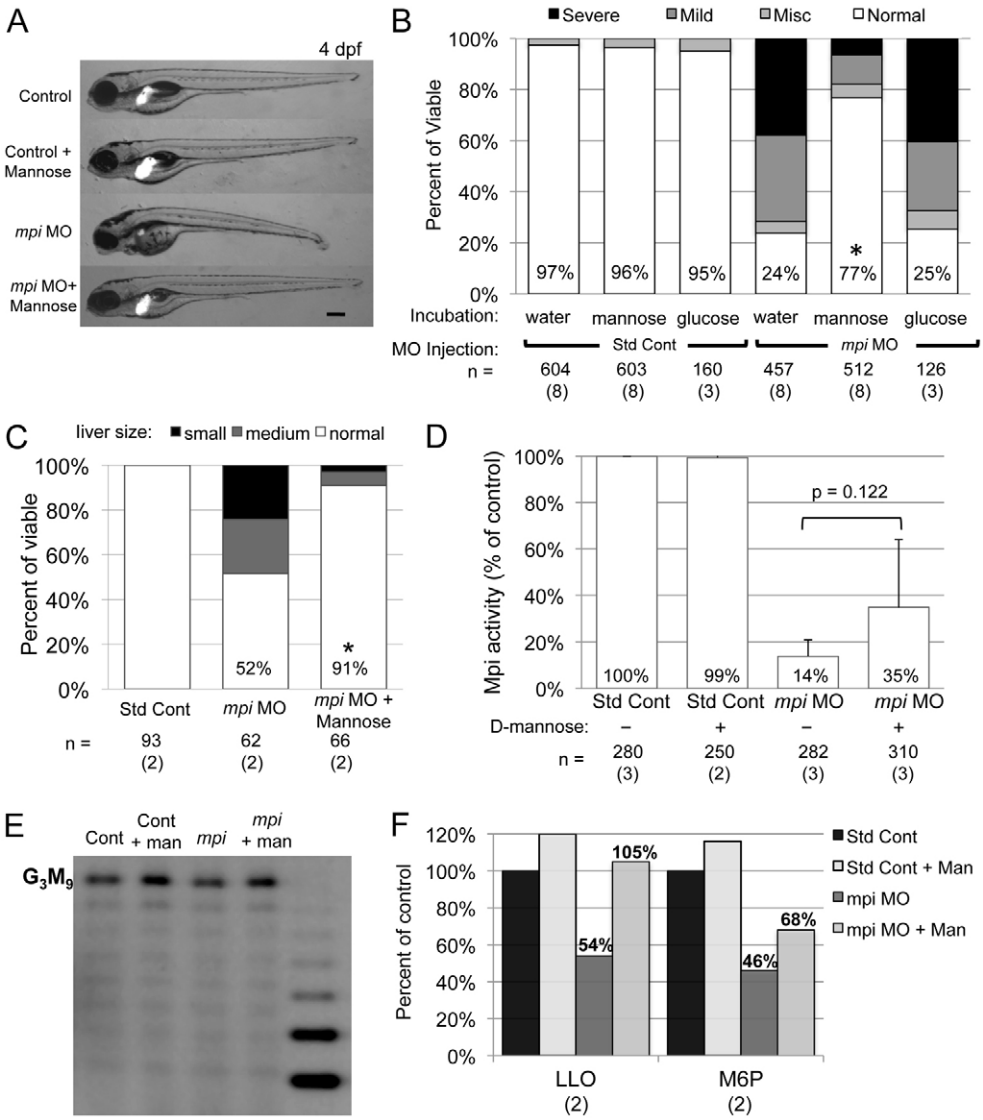

Fig. 5. Mannose supplementation rescues *mpi* morphants. (A) Phenotype rescue of *mpi* morphants treated with 50 mM mannose at 4 dpf. Liver visualized using *Tg(fabp10*:dsRed*)*. Scale bar: 100 µm. (B) 77% of *mpi* morphants treated with 50 mM mannose from fertilization through 4 dpf appear completely normal, whereas no rescue is seen with glucose. **P*<0.0001 by Fisher's exact test as compared with *mpi* MO + water or *mpi* MO + glucose supplementation. (C) Liver size is improved in *mpi* morphants treated with mannose supplementation. **P*<0.0001 by Fisher's exact test. (D) Mpi activity is not significantly changed with mannose supplementation. (E) FACE analysis with quantification showing restoration of G_3M_9 LLO levels in *mpi* morphants treated with mannose as compared with *mpi* MO alone. Average of two experiments. (F) LLO and M6P levels are increased in *mpi* morphants treated with mannose to 105% and 68%, respectively. Average of two experiments. Numbers in parentheses under *n* values indicate the number of experiments.

that these effects can be rescued by mannose supplementation, as seen in patients.

MPI enzyme is essential early in the N-glycosylation pathway, as well as for all other mannosyl glycoconjugates, converting fructose-6-phosphate to mannose-6-phosphate. Uniquely, oral mannose supplements increase flux through a minor complementary metabolic pathway to produce mannose-6-phosphate, enabling LLO synthesis and augmenting protein glycosylation that results in resolution of most symptoms for MPI-CDG patients. By using *mpi* morpholino knockdown, we can precisely decrease Mpi enzyme activity to levels corresponding to that of MPI-CDG patients. Our *mpi* morphants also demonstrate LLO deficiencies as well as multi-systemic phenotypes, specific to Mpi loss, as demonstrated by *mpi* mRNA rescue.

Individuals with MPI-CDG are unusual in that they do not have intellectual disability or neurological impairment, compared with most other type I disorders, especially PMM2-CDG (Freeze et al., 2012). A possible explanation for this difference is that circulating maternal mannose in mammals is sufficient to prevent some developmental defects in MPI-CDG prenatally, whereas this does not have any effect when PMM2 is deficient because there is no complementary metabolic pathway that can create sufficient levels of the PMM2 product, mannose-1-phosphate. We speculate that adding mannose to the zebrafish water could simulate circulating maternal mannose. Were it not for maternal mannose, individuals with MPI-CDG might be as neurologically impaired as those with PMM2-CDG, as suggested by the severe brain abnormalities observed in *mpi* morphants.

MPI-CDG is known as the 'gastrointestinal type' of CDG because affected individuals present with diarrhea, hepatic fibrosis and coagulopathy caused by defective hepatocyte secretion of clotting factors. *mpi* morphants display abnormal liver development. Additionally, preliminary experiments indicate that *mpi* morphants have an increase in a marker of hepatic stellate cells (Yin et al., 2012), the cells responsible for generating the scar that forms in hepatic fibrosis (Chunyue Yin, personal communication). Thus, *mpi* morphants promise to be useful for investigating the basis of liver disease caused by Mpi deficiency.

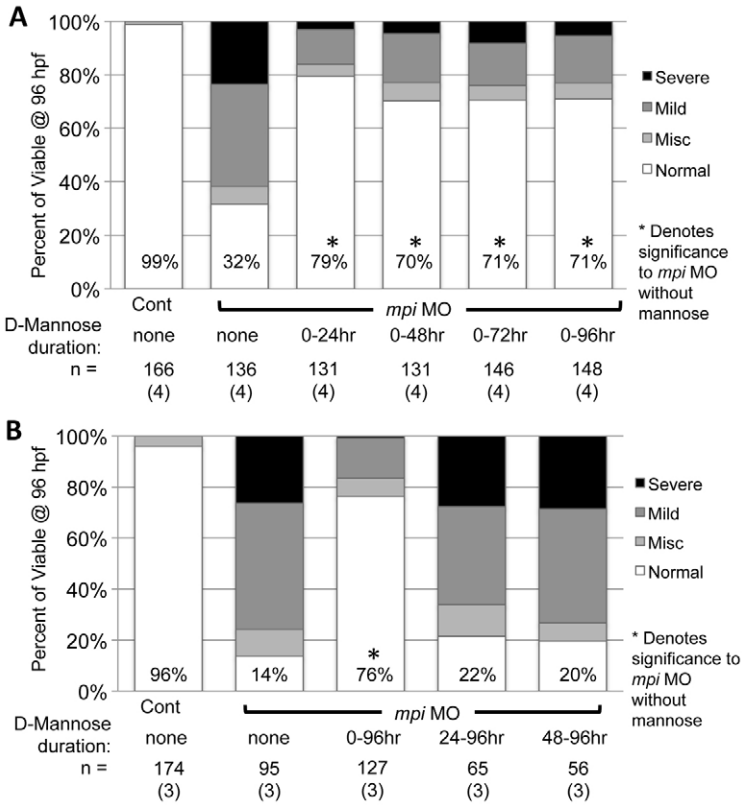

Fig. 6. Embryonic rescue is only effective with mannose supplementation early in development. (A) Time course of mannose removal. Mannose was added to control and *mpi* MO embryos at 1 hpf and then subsequently removed at 24, 48 or 72 hpf, or not removed at all until scored at 96 hpf. **P*<0.0001, 0.0003, 0.0003 and 0.0001, respectively, by Fisher's exact test compared with *mpi* MO alone. (B) Time course of mannose addition. Mannose was added to control and *mpi* MO embryos at 0, 24 or 48 hpf. Significant rescue only occurred in embryos in which mannose was added at 0 hpf (**P*<0.0001 by Fisher's exact test), whereas no rescue was seen in embryos where mannose was added at 24 hpf or at 48 hpf (*P*=0.2045 and 0.3624, respectively, by Fisher's exact test). Numbers in parentheses under *n* values indicate the number of experiments.

In addition, *mpi* morphants have multi-systemic defects, including defects of the eye, forebrain, heart, tail and jaw, at 4 dpf. This phenotypic discrepancy might be a result of the ability to examine zebrafish embryos deficient in Mpi during the period of embryogenesis, whereas these defects are not diagnosed until after birth in humans and might represent the milder spectrum of MPI-CDG patients. Mammalian embryos with multi-systemic defects, like those we see in our embryos, are probably incompatible with term birth. The early embryonic lethality of mouse *Mpi*$^{-/-}$ embryos at E11.5 (DeRossi et al., 2006) further suggests that low levels of Mpi are not compatible with survival through early development. We previously demonstrated that blocking protein glycosylation in zebrafish larvae with tunicamycin results in a pronounced hepatic phenotype (fatty liver) (Cinaroglu et al., 2011). However, there is a marked difference between inhibiting glycosylation later in development (tunicamycin is added at 3 dpf) and the global decrease in Mpi activity effective from the onset of embryogenesis as achieved in our *mpi* morphants. Indeed, our preliminary data demonstrate that treating early embryos with tunicamycin results in lethality and defects that resemble *mpi* morphants (not shown).

The simple addition of mannose to fish water, akin to supplementation in MPI-CDG patients, results in remarkable rescue of the *mpi* morphant phenotype, including improvement in liver development, and not only confirms the specificity of phenotype but validates the zebrafish as a tool to study MPI-CDG and potentially other disorders of glycosylation. Interestingly, our mannose experiments revealed a small window of optimal mannose supplementation at the earliest time in development: mannose was only effective if provided prior to 24 hpf. This points to crucial, early developmental events dependent on Mpi and suggests that an absence of mannose supplementation early in development might manifest later as defects, including irreversible defects such as liver fibrosis, that are actual consequences of early Mpi dysfunction. Another possibility accounting for the lack of rescue with later mannose supplementation is altered permeability or decreased utilization of mannose by the maturing embryo.

Our initial mannose titration experiments showed increased mannose-6-phosphate levels upon mannose treatment of control embryos, but no decrease in LLO levels (supplementary material Fig. S4). Recently, we reported with permeabilized and cultured mammalian cells that mannose-6-phosphate can promote LLO hydrolysis and that this reaction can deplete steady-state LLO levels if the rate of loss is greater than the rate of LLO resynthesis (Gao et al., 2011; Gao et al., 2005). In contrast, LLO levels are stable despite active LLO hydrolysis if biosynthetic conditions are favorable. Mannose-treated zebrafish that accumulated mannose-6-phosphate also accumulated free glycans, a hallmark of mannose-6-phosphate-dependent LLO hydrolysis, to ~160-170% of levels in untreated fish (not shown). It would appear, therefore, that LLO synthesis in mannose-treated zebrafish is robust, and able to overcome any loss due to increased concentrations of mannose-6-phosphate.

Although the biochemical and phenotypic defects in individuals with CDG are well described, the pathophysiology remains largely unknown. The enzymatic deficiencies caused by hypomorphic mutations could result in substrate build up, product absence, or a cellular response to abnormal glycosylation of a single protein in a single cell type or of a complex set of proteins in all cells. One possibility of the latter case is that abnormal protein glycosylation results in protein misfolding and resultant endoplasmic reticulum

stress (Shang et al., 2002). Our preliminary analysis did not reveal any induction of genes targeted by the unfolded protein response (not shown), a pathway that becomes activated when hypoglycosylated and unfolded proteins accumulate in the endoplasmic reticulum, making this an unlikely explanation of the *mpi* morphant phenotype. An alternative possibility is that abnormal protein glycosylation creates a signal that induces apoptosis, a commonly observed phenotype in cells treated with tunicamycin. Cell death could cause failed organ development and small embryos size. We indeed see increased cell death in *mpi*-morpholino-injected embryos (not shown); however, determining whether this is apoptosis and whether this accounts for the *mpi* morphant phenotype requires further investigation.

Our zebrafish model represents the first free-living in vivo model to study MPI-CDG and sets the proof-of-principle to use zebrafish to study other CDG and disorders of glycosylation. We hope that this might serve as a platform to further investigate the pathophysiology underlying this set of disorders and, ultimately, to utilize these zebrafish models for therapeutic screening.

METHODS

Zebrafish maintenance and embryo injection

Adult zebrafish were maintained on a 14:10 hour light:dark cycle at 28°C. Wild-type (WT; AB and Tab 14) and *Tg(fabp10:dsRed)* fish were used. Fertilized embryos collected following natural spawning were cultured at 28°C in fish water (0.6 g/l Crystal Sea Marinemix; Marine Enterprises International, Baltimore, MD) containing methylene blue (0.002 g/l). The Mount Sinai School of Medicine Institutional Animal Care and Use Committee approved all protocols.

A morpholino (5′-ATGGCGGAAGTGAAAGTGTTTCCTC-3′) targeting the ATG (underlined) of the *mpi* transcript, and a standard control morpholino (5′-CCTCTTACCTCAGTTA-CAATTTATA-3′) that does not target any known zebrafish transcript were obtained from Gene Tools (Philomath, OR). Needles were calibrated to inject 4 nl per embryo using a Narishige IM-300 microinjector; 6.7 ng of morpholino per embryo was identified as optimal. The same volume of injection was used for introducing 2 ng of mRNA encoding 6×-Myc-tagged zebrafish Mpi (6×Myc-Mpi). All injections were carried out in one- to four-cell-stage embryos.

Mannose treatment

Zebrafish embryos were treated with 50 mM D-mannose (Sigma) in fish water starting at 30-60 minutes post-fertilization, and the mannose-containing water was refreshed at 24 and 48 hours. Larvae were collected and scored at 4 dpf. For time-course studies, mannose was either added or removed at 24, 48 or 72 hpf and were scored at 96 hpf (i.e. 4 dpf). Larvae were treated with tunicamycin as previously described (Cinaroglu et al., 2011).

Preparation of zebrafish extracts and enzyme assay

Zebrafish larvae were homogenized in 50 mM HEPES pH 7.4 [without EDTA and with protease inhibitors (Roche)] and lysed by sonication followed by centrifugation at 20,817 ***g*** for 10 minutes at 4°C. Protein concentration of the supernatant was determined by the Bradford assay (Bradford, 1976). A coupled assay using phosphoglucose isomerase and glucose-6-phosphate dehydrogenase with NADPH measured by spectrophotometric analysis at 340 nm was used to assay MPI and PMM2 activities as described (Van Schaftingen and Jaeken, 1995). Modifications included using a final volume of 1 ml and enzyme activity was measured in a 96-well plate for 20 minutes using a FLUOstar Omega microplate reader (BMG LABTECH). Samples were measured 20 minutes after adding the substrate. Units were calculated as mU of enzyme activity/mg of protein based on the change in OD during a 20-minute reaction time.

Cloning

A clone encoding the cDNA of zebrafish *mpi* was obtained from Open Biosystems (Genbank Accession NM_001033110). The coding sequence was amplified by PCR using degenerate primers surrounding the ATG to create significant mismatch with the *mpi* morpholino (supplementary material Table S1). This was subcloned using the pCR8/GW/TOPO TA Cloning Kit (Invitrogen, Carlsbad, CA) used in combination with Gateway compatible vectors to create an mRNA expression vector appropriate for zebrafish embryos (Villefranc et al., 2007) encoding six copies of a Myc-tag at the N-terminus of Mpi (pCS3-6×MT-Mpi).

Phenotype scoring

All embryos were scored for phenotypic abnormalities on 4 dpf. Although most clutches of uninjected or control-injected larvae had a few larvae that displayed a range of phenotypes that deviated from the appearance of healthy larvae, which we labeled as 'normal', the morphological defects in *mpi* morphants were specific, consistent and relatively homogeneous within two distinct groups, which we labeled as 'mild' or 'severe' phenotypes. The equation in Fig. 3D describes the calculation of the 'phenotype score', which reflects the overall phenotypic severity of the clutch: the number of normal larvae was multiplied by a factor of 1, mild larvae by a factor of 2 and severe larvae by a factor of 3, and the sum of these were divided by the total number of viable larvae. Thus, a clutch with 100% of larvae displaying a severely affected *mpi* morphant phenotype would have a score of 3 and a clutch in which all the larvae were normal would have a score of 1. This enabled quantification of clutch-to-clutch variation and correlation of the range in severity of a clutch to the degree of residual Mpi enzyme activity. Linear regression analysis shows that the phenotype score is linearly and inversely correlated with residual Mpi enzyme activity (R^2=0.87; Fig. 3E).

mRNA rescue

mRNA encoding zebrafish Mpi was produced by linearization of the pCS3-6×MT-Mpi vector with *Nsi*I and capped mRNA was synthesized using mMessage mMachine (Ambion, USA). mRNA was purified using lithium chloride, diluted in RNase free water, and either injected 4 nl alone at a concentration of 500 ng/µl or co-injected with 6.7 ng of *mpi* morpholino into embryos within 1 hpf.

Western blots

Protein lysates were prepared from ten larvae on 4 dpf by homogenization in lysis buffer (20 mM Tris pH 7.5, 150 mM NaCl, 1% NP-40, 2 mM EDTA, 10% glycerol and protease inhibitors). Lysates were centrifuged and 1:5 volume of sample buffer was added to the supernatant to achieve 2% SDS, 5% 2-mercaptoethanol. Anti-

myc (9E10 at 1:1500; Abgent) and anti-tubulin (1:2000; Developmental Studies Hybridoma Bank) were used.

FACE analysis

A total of 70-100 embryos collected at 4 dpf were added to 1 ml of methanol at room temperature, followed by brief sonication, and then transferred into a 15-ml conical tube with an additional 8-10 ml of methanol. LLOs, total N-glycan pools and sugar phosphates were identified and quantified as described (Gao and Lehrman, 2006). Results were normalized to protein measured in the embryo samples. Fluorescent saccharides were quantified with a Bio-Rad Fluor-S scanner equipped with Quantity-One software.

Mannose-6-phosphate assay

Zebrafish extract was prepared according to Donthi and Epstein (Donthi and Epstein, 2007). Briefly, 1 M perchloric acid (150 ml) was added to 30 zebrafish embryos (4 dpf) and sonication conducted for 10 seconds on ice followed by centrifugation at 15,294 ***g*** for 5 minutes at 4°C. Acid was neutralized with dropwise addition of 2 M potassium bicarbonate (150 ml). Precipitated salt was removed by another centrifugation at 15,294 ***g*** for 5 minutes at 4°C. A total of 10 ml of the supernatant per well was used for mannose-6-phosphate determination. The coupled enzyme assay was modified from Zhu et al. (Zhu et al., 2009), whereby mannose-6-phosphate is the limiting substrate, which is converted to glucose-6-phosphate using a series of enzymes with a final fluorescence readout. Briefly, 10 ml deionized water and 10 ml zebrafish extract of each sample was added to wells of a black assay plate. Depending on the number of samples, two sets of reaction mix were prepared containing 50 mM HEPES, 1 mM magnesium chloride, 100 mM NADP, 10 mM resazurin, 0.25 units diaphorase in a total volume of 80 ml per sample. Phosphomannose isomerase, phosphoglucose isomerase and glucose-6-phosphate dehydrogenase (0.25 units each/sample) were added to one set (F3) and only phosphoglucose isomerase and glucose-6-phosphate dehydrogenase (0.25 units each/sample) were added to the other set (F2). Another mix (Fb), containing glucose-6-phosphate dehydrogenase but devoid of NADP, was prepared to determine the background caused by the endogenous NADP in each sample. 80 ml of the mix was added to the wells containing 20 ml of the extract. After 15 minutes, fluorescence was recorded at excitation wavelength 530 nm and emission at 590 nm using Flexstation III (Molecular Devices, Sunnyvale, CA). Background fluorescence (Fb) was subtracted from F3 and F2 and the difference between the fluorescence values (F3–F2) was used to calculate mannose-6-phosphate based on a standard curve generated by known amounts of G6P in 20 ml deionized water and 80 µl of reaction mix containing only glucose-6-phosphate dehydrogenase.

COMPETING INTERESTS

The authors declare that they do not have any competing or financial interests.

AUTHOR CONTRIBUTIONS

J.C., R.S., H.H.F., M.A.L. and K.C.S. conceived and designed the experiments. J.C., A.M., N.G., S.R., C.M. and V.S. performed the experiments. J.C., A.M., N.G., V.S., R.S., H.H.F., M.A.L. and K.C.S. analyzed the data. J.C. and K.C.S. wrote the paper.

FUNDING

Funded by National Institutes of Health-American Recover and Reinvestment Act [RC1 HD064159]; and National Institutes of Health [K12 HD052890-0510 to J.C., GM38545 to M.A.L., R01-GM-086524 to R.S., R01AA018886 to K.C.S.]; Welch Foundation [I-1168 to M.A.L.]; and The Rocket Fund to H.H.F.

SUPPLEMENTARY MATERIAL

Supplementary material for this article is available at http://dmm.biologists.org/lookup/suppl/doi:10.1242/dmm.010116/-/DC1

REFERENCES

Babovic-Vuksanovic, D., Patterson, M. C., Schwenk, W. F., O'Brien, J. F., Vockley, J., Freeze, H. H., Mehta, D. P. and Michels, V. V. (1999). Severe hypoglycemia as a presenting symptom of carbohydrate-deficient glycoprotein syndrome. *J. Pediatr.* **135**, 775-781.

Blomme, B., Van Steenkiste, C., Callewaert, N. and Van Vlierberghe, H. (2009). Alteration of protein glycosylation in liver diseases. *J. Hepatol.* **50**, 592-603.

Bradford, M. M. (1976). A rapid and sensitive method for the quantitation of microgram quantities of protein utilizing the principle of protein-dye binding. *Anal. Biochem.* **72**, 248-254.

Chu, J. and Sadler, K. C. (2009). New school in liver development: lessons from zebrafish. *Hepatology* **50**, 1656-1663.

Cinaroglu, A., Gao, C., Imrie, D. and Sadler, K. C. (2011). Activating transcription factor 6 plays protective and pathological roles in steatosis due to endoplasmic reticulum stress in zebrafish. *Hepatology* **54**, 495-508.

Damen, G., de Klerk, H., Huijmans, J., den Hollander, J. and Sinaasappel, M. (2004). Gastrointestinal and other clinical manifestations in 17 children with congenital disorders of glycosylation type Ia, Ib, and Ic. *J. Pediatr. Gastroenterol. Nutr.* **38**, 282-287.

de Koning, T. J., Dorland, L., van Diggelen, O. P., Boonman, A. M., de Jong, G. J., van Noort, W. L., De Schryver, J., Duran, M., van den Berg, I. E., Gerwig, G. J. et al. (1998). A novel disorder of N-glycosylation due to phosphomannose isomerase deficiency. *Biochem. Biophys. Res. Commun.* **245**, 38-42.

de Lonlay, P. and Seta, N. (2009). The clinical spectrum of phosphomannose isomerase deficiency, with an evaluation of mannose treatment for CDG-Ib. *Biochim. Biophys. Acta* **1792**, 841-843.

de Lonlay, P., Cuer, M., Vuillaumier-Barrot, S., Beaune, G., Castelnau, P., Kretz, M., Durand, G., Saudubray, J. M. and Seta, N. (1999). Hyperinsulinemic hypoglycemia as a presenting sign in phosphomannose isomerase deficiency: A new manifestation of carbohydrate-deficient glycoprotein syndrome treatable with mannose. *J. Pediatr.* **135**, 379-383.

DeRossi, C., Bode, L., Eklund, E. A., Zhang, F., Davis, J. A., Westphal, V., Wang, L., Borowsky, A. D. and Freeze, H. H. (2006). Ablation of mouse phosphomannose isomerase (Mpi) causes mannose 6-phosphate accumulation, toxicity, and embryonic lethality. *J. Biol. Chem.* **281**, 5916-5927.

Donthi, R. V. and Epstein, P. N. (2007). Altering and analyzing glucose metabolism in perfused hearts of transgenic mice. *Methods Mol. Med.* **139**, 151-161.

Ekker, S. C. and Larson, J. D. (2001). Morphant technology in model developmental systems. *Genesis* **30**, 89-93.

Freeze, H. H. (2001). Congenital disorders of glycosylation and the pediatric liver. *Semin. Liver Dis.* **21**, 501-515.

Freeze, H. H. (2006). Genetic defects in the human glycome. *Nat. Rev. Genet.* **7**, 537-551.

Freeze, H. H. (2009). Towards a therapy for phosphomannomutase 2 deficiency, the defect in CDG-Ia patients. *Biochim. Biophys. Acta* **1792**, 835-840.

Freeze, H. H., Eklund, E. A., Ng, B. G. and Patterson, M. C. (2012). Neurology of inherited glycosylation disorders. *Lancet Neurology* **11**, 453-466.

Gao, N. and Lehrman, M. A. (2006). Non-radioactive analysis of lipid-linked oligosaccharide compositions by fluorophore-assisted carbohydrate electrophoresis. *Methods Enzymol.* **415**, 3-20.

Gao, N., Shang, J. and Lehrman, M. A. (2005). Analysis of glycosylation in CDG-Ia fibroblasts by fluorophore-assisted carbohydrate electrophoresis: implications for extracellular glucose and intracellular mannose 6-phosphate. *J. Biol. Chem.* **280**, 17901-17909.

Gao, N., Shang, J., Huynh, D., Manthati, V. L., Arias, C., Harding, H. P., Kaufman, R. J., Mohr, I., Ron, D., Falck, J. R. et al. (2011). Mannose-6-phosphate regulates destruction of lipid-linked oligosaccharides. *Mol. Biol. Cell* **22**, 2994-3009.

Gill, A., Gao, N. and Lehrman, M. A. (2002). Rapid activation of glycogen phosphorylase by the endoplasmic reticulum unfolded protein response. *J. Biol. Chem.* **277**, 44747-44753.

Haeuptle, M. A. and Hennet, T. (2009). Congenital disorders of glycosylation: an update on defects affecting the biosynthesis of dolichol-linked oligosaccharides. *Hum. Mutat.* **30**, 1628-1641.

Harms, H. K., Zimmer, K. P., Kurnik, K., Bertele-Harms, R. M., Weidinger, S. and Reiter, K. (2002). Oral mannose therapy persistently corrects the severe clinical symptoms and biochemical abnormalities of phosphomannose isomerase deficiency. *Acta Paediatr.* **91**, 1065-1072.

Hendriksz, C. J., McClean, P., Henderson, M. J., Keir, D. G., Worthington, V. C., Imtiaz, F., Schollen, E., Matthijs, G. and Winchester, B. G. (2001). Successful treatment of carbohydrate deficient glycoprotein syndrome type 1b with oral mannose. *Arch. Dis. Child.* **85**, 339-340.

Jaeken, J. (2010). Congenital disorders of glycosylation. *Ann. N. Y. Acad. Sci.* **1214**, 190-198.

Jaeken, J., Vanderschueren-Lodeweyckx, M., Casaer, P., Snoeck, L., Corbeel, L., Eggermont, E. and Eeckels, R. (1980). Familial psychomotor retardation with markedly fluctuating serum prolactin, FSH and GH levels, partial TBG-deficiency, increased serum arylsulphatase A and increased CSF protein: a new syndrome? (Abstract). *Pediat. Res.* **14**, 179.

Jaeken, J., Matthijs, G., Saudubray, J. M., Dionisi-Vici, C., Bertini, E., de Lonlay, P., Henri, H., Carchon, H., Schollen, E. and Van Schaftingen, E. (1998). Phosphomannose isomerase deficiency: a carbohydrate-deficient glycoprotein syndrome with hepatic-intestinal presentation. *Am. J. Hum. Genet.* **62**, 1535-1539.

Kjaergaard, S. (2004). Congenital disorders of glycosylation type Ia and Ib. Genetic, biochemical and clinical studies. *Dan. Med. Bull.* **51**, 350-363.

Kornfeld, R. and Kornfeld, S. (1985). Assembly of asparagine-linked oligosaccharides. *Annu. Rev. Biochem.* **54**, 631-664.

Lieschke, G. J. and Currie, P. D. (2007). Animal models of human disease: zebrafish swim into view. *Nat. Rev. Genet.* **8**, 353-367.

Mention, K., Lacaille, F., Valayannopoulos, V., Romano, S., Kuster, A., Cretz, M., Zaidan, H., Galmiche, L., Jaubert, F., de Keyzer, Y. et al. (2008). Development of liver disease despite mannose treatment in two patients with CDG-Ib. *Mol. Genet. Metab.* **93**, 40-43.

Miller, B. S., Khosravi, M. J., Patterson, M. C. and Conover, C. A. (2009). IGF system in children with congenital disorders of glycosylation. *Clin. Endocrinol.* **70**, 892-897.

Mudbhary, R. and Sadler, K. C. (2011). Epigenetics, development, and cancer: zebrafish make their ARK. *Birth Defects Res. C Embryo Today* **93**, 194-203.

Niehues, R., Hasilik, M., Alton, G., Korner, C., Schiebe-Sukumar, M., Koch, H. G., Zimmer, K. P., Wu, R., Harms, E., Reiter, K. et al. (1998). Carbohydrate-deficient glycoprotein syndrome type Ib. Phosphomannose isomerase deficiency and mannose therapy. *J. Clin. Invest.* **101**, 1414-1420.

Penel-Capelle, D., Dobbelaere, D., Jaeken, J., Klein, A., Cartigny, M. and Weill, J. (2003). Congenital disorder of glycosylation Ib (CDG-Ib) without gastrointestinal symptoms. *J. Inherit Metab. Dis.* **26**, 83-85.

Robu, M. E., Larson, J. D., Nasevicius, A., Beiraghi, S., Brenner, C., Farber, S. A. and Ekker, S. C. (2007). p53 activation by knockdown technologies. *PLoS Genet.* **3**, e78.

Shang, J., Korner, C., Freeze, H. and Lehrman, M. A. (2002). Extension of lipid-linked oligosaccharides is a high-priority aspect of the unfolded protein response: endoplasmic reticulum stress in Type I congenital disorder of glycosylation fibroblasts. *Glycobiology* **12**, 307-317.

Thisse, B. and Thisse, C. (2004). Fast release clones: a high throughput expression analysis. *ZFIN Direct Data Submission (http://zfin. org)*.

Van Schaftingen, E. and Jaeken, J. (1995). Phosphomannomutase deficiency is a cause of carbohydrate-deficient glycoprotein syndrome type I. *FEBS Lett.* **377**, 318-320.

Villefranc, J. A., Amigo, J. and Lawson, N. D. (2007). Gateway compatible vectors for analysis of gene function in the zebrafish. *Dev. Dyn.* **236**, 3077-3087.

Westphal, V., Kjaergaard, S., Davis, J. A., Peterson, S. M., Skovby, F. and Freeze, H. H. (2001). Genetic and metabolic analysis of the first adult with congenital disorder of glycosylation type Ib: long-term outcome and effects of mannose supplementation. *Mol. Genet. Metab.* **73**, 77-85.

Yin, C., Evason, K. J., Maher, J. J. and Stainier, D. Y. (2012). The bHLH transcription factor Hand2 marks hepatic stellate cells in zebrafish: Analysis of stellate cell entry into the developing liver. *Hepatology* doi:10.1002/hep.25757.

Zhu, A., Romero, R. and Petty, H. R. (2009). An enzymatic fluorimetric assay for glucose-6-phosphate: application in an in vitro Warburg-like effect. *Anal. Biochem.* **388**, 97-101.

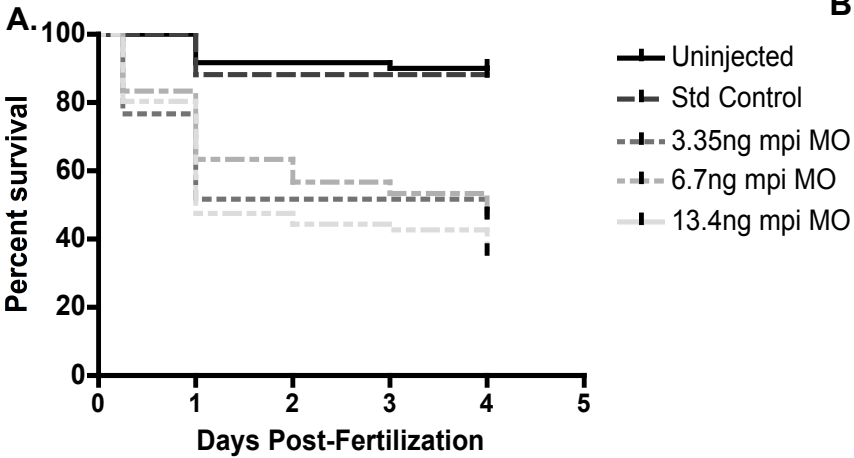

B.

	cumulative survival (to 4 dpf)
Uninjected	90%
Std Cont	88%
3.35ng *mpi* MO	47%
6.7ng *mpi* MO	47%
13.4ng *mpi* MO	36%

Figure S1. *mpi* morphants have worse survival with increased Mpi knockdown. A.) Kaplan-Meier curve of uninjected embryos as compared to embryos injected with standard control MO and increasing amounts of *mpi* MO. N = 60 embryos for all groups at time of injection. **B.)** Cumulative survival by 4 dpf of larvae scored in panel A.

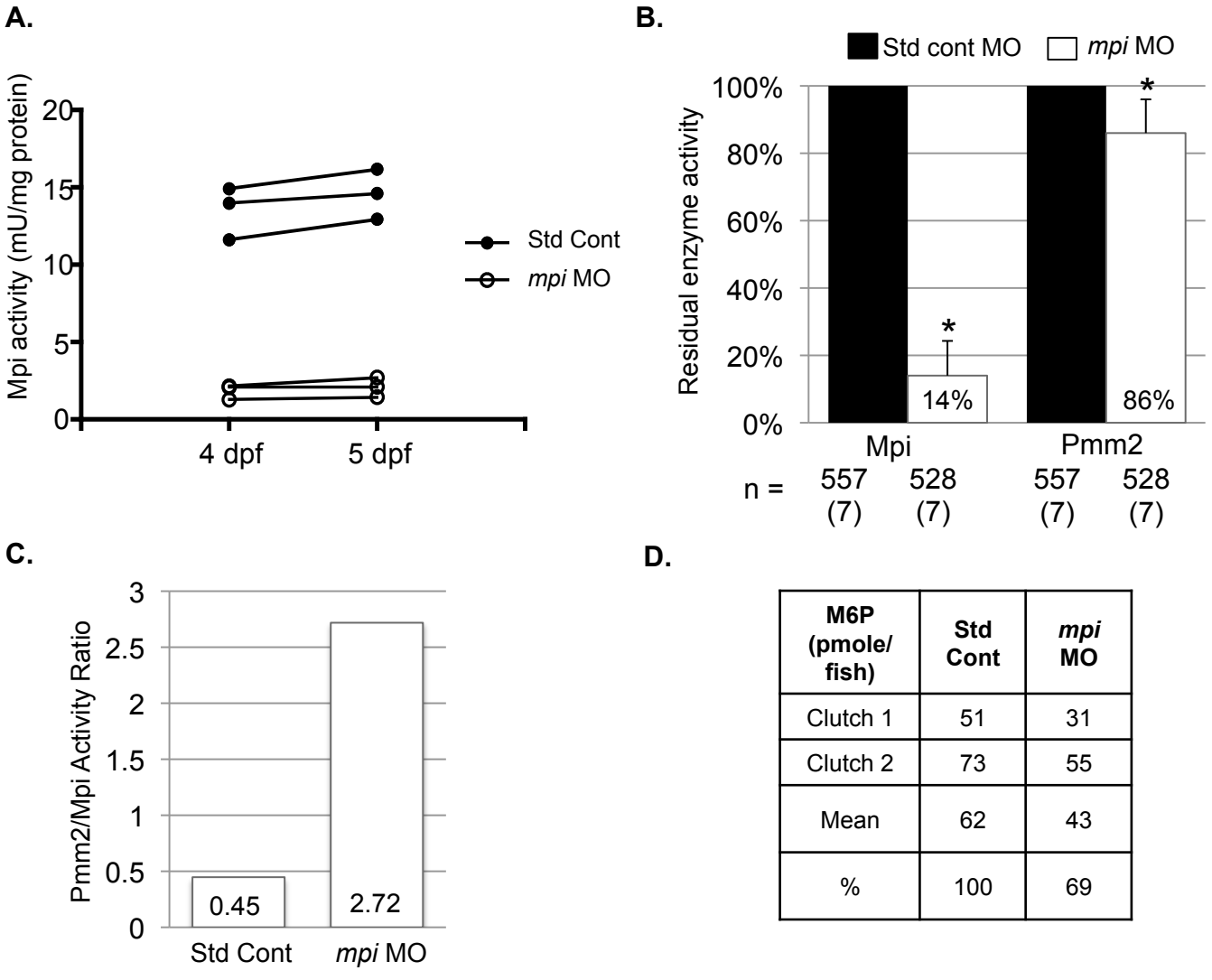

M6P (pmole/ fish)	Std Cont	*mpi* MO
Clutch 1	51	31
Clutch 2	73	55
Mean	62	43
%	100	69

Figure S2. *mpi* morpholino specifically depletes Mpi activity and decreases mannose 6-phosphate. A.) Mpi activity does not significantly change from in 4 dpf compared to 5 dpf in *mpi* morphant embryos ($p = 0.71$ by paired T-test). **B.)** Mpi and Pmm2 enzyme activity are significantly decreased in *mpi* MO ($p=8.27861E-06$ and 0.048, respectively, by paired T-test). **C.)** Pmm2/Mpi activity ratio is increased in *mpi* morphants. Average of mU/mg of protein for 7 experiments. **D.)** Standard coupled assay for M6P demonstrates that 4 dpf *mpi* morphants have only 69% of M6P compared to controls. Results from 2 experiments are shown.

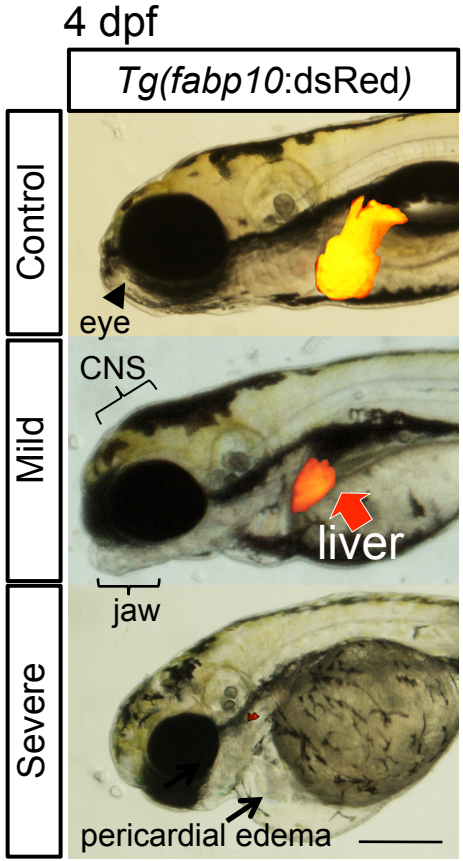

Figure S3. *mpi* morphants show multisystemic defects, including abnormal liver development as visualized in *Tg(fabp10:dsRed)* embryos at 4 dpf. Scale bar = 500 microns.

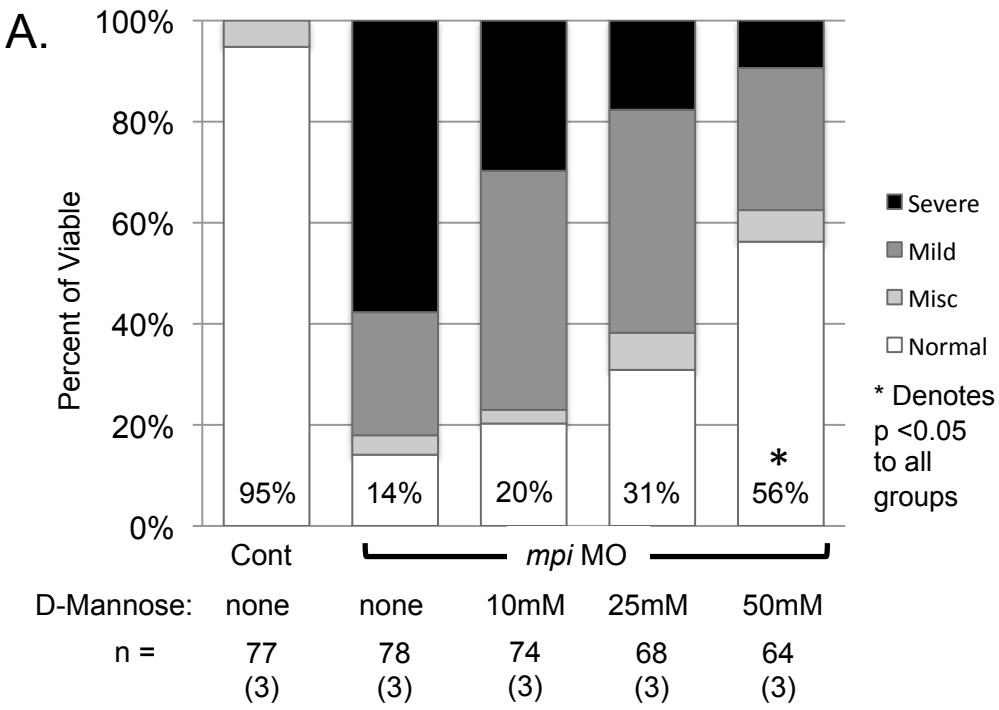

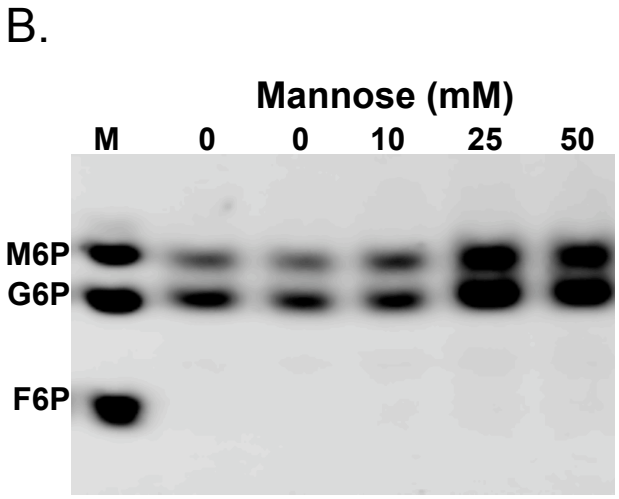

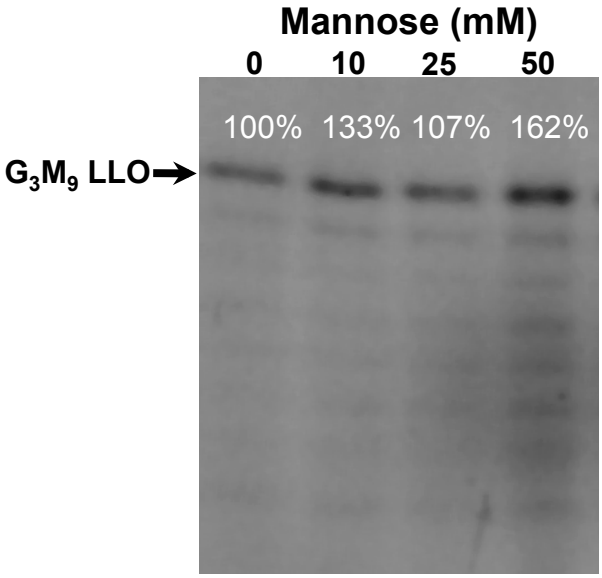

Figure S4. Mannose titration shows increased rescue of *mpi* MO phenotype, increased M6P levels, and no degradation of LLO levels. A.) Phenotypic scoring of control and *mpi* MO injected embryos treated with increasing concentrations of D-mannose from 0 to 96 hpf. **B.)** M6P levels increase in control embryos treated with increasing mannose concentrations from 0 to 50mM. **C.)** FACE analysis showing no degradation of G_3M_9 LLO with increasing concentrations of mannose from 0 to 50mM.

Table S1. Cloning primers

zmpi_degenerate_Fwd	5’-GC**C**GA**G**GT**C**AA**G**GTGTTTCCTCTGTGCTGT-3’
ATG MO Seq	ATGGCGGAAGTGAAAGTGTTTCCTC
zmpi	CGTTGCAGACATGGCGGAAGTGAAAGTGTT

Bases in bold represent introduced degeneracy.

	Uninjected	Standard Control MO	0.34ng *mpi* MO	3.35ng *mpi* MO	6.70ng *mpi* MO
Mpi Enzyme Activity (mU/mg of protein)	11.13	14.60	10.77	3.24	2.16
	12.87	12.24	10.22	3.28	0.93
	13.62	16.05	11.13	2.25	1.86
	18.79	12.38		3.44	2.39
	13.64	10.60			1.02
		16.07			1.00
		13.62			1.29
		18.79			0.33
		14.33			3.80
		13.98			2.64
		7.17			2.01
		15.32			2.16
		12.24			2.09
		16.70			1.88
Mean	14.02	13.86	10.71	3.05	1.83
Median	13.62	14.16	10.77	3.26	1.95
Standard Deviation	2.86	2.88	0.46	0.54	0.87
Percent of Control	101.06%	100.00%	77.23%	22.02%	13.17%
P=	0.92	-	1.50E-3	7.94E-10	1.43E-10

Table S2. Mpi specific sctivity (mU/mg protein) shown for all clutches of embryos injected with standard control MO or increasing *mpi* MO amounts.